J. Fluid Mech. (1983), *vol.* 135, *pp.* 95–110
Printed in Great Britain

Gravity currents produced by instantaneous releases of a heavy fluid in a rectangular channel

By JAMES W. ROTTMAN AND JOHN E. SIMPSON
Department of Applied Mathematics and Theoretical Physics, University of Cambridge, Silver Street, Cambridge CB3 9EW

(Received 9 February 1983 and in revised form 6 July 1983)

Results of laboratory experiments are presented in which a finite volume of homogeneous fluid was released instantaneously into another fluid of slightly lower density. The experiments were performed in a channel of rectangular cross-section, and the two fluids used were salt water and fresh water. As previously reported, the resulting gravity current, if viscous effects are negligible, passes through two distinct phases: an initial adjustment phase, during which the initial conditions are important, and an eventual self-similar phase, in which the front speed decreases as $t^{-\frac{1}{3}}$ (where t is the time measured from release). The experiments reported herein were designed to emphasize the inviscid motion. From our observations we argue that the current front moves steadily in the first phase, and that the transition to the inviscid self-similar phase occurs when a disturbance generated at the endwall (or plane of symmetry) overtakes the front. If the initial depth of the heavy fluid is equal to or slightly less than the total depth of the fluid in the channel, the disturbance has the appearance of an internal hydraulic drop. Otherwise, the disturbance is a long wave of depression. Measurements of the duration of the initial phase and of the speed and depth of the front during this phase are presented as functions of the ratio of the initial heavy fluid depth to the total fluid depth. These measurements are compared with numerical solutions of the shallow-water equations for a two-layer fluid.

1. Introduction

A gravity current (sometimes called a density current or buoyancy current) is formed by fluid flowing mainly horizontally under the influence of gravity into another fluid of different density. A common procedure for generating gravity currents in the laboratory is the sudden removal of a vertical barrier separating two fluids of different densities in a channel. Using this technique with salt water and fresh water as the two fluids, O'Brien & Cherno (1934), Yih (1947), Keulegan (1957), Barr (1967), Simpson & Britter (1979) and Huppert & Simpson (1980) have produced gravity currents in channels of rectangular cross-section. In most of these experiments the volume of one of the fluids was much smaller than that of the other, so the experiments approximate the release of a finite volume of fluid into another fluid of infinite volume.

From the results of these experiments and those of our own it appears that the gravity current produced by an instantaneous release passes through two distinct phases, if viscous effects are negligible. There is an initial adjustment phase, during which the initial conditions are important, and an eventual self-similar phase in which the front speed decreases as $t^{-\frac{1}{3}}$ (where t is the time measured from release). The transition from the first to the second phase is observed to be rather abrupt.

Theories for gravity current motion resulting from instantaneous releases have been proposed by Fay (1969), Fannelop & Waldman (1972), Hoult (1972) and Huppert & Simpson (1980). All these theories predict that the front speed eventually will decrease as $t^{-\frac{1}{3}}$, based on the assumption that the motion is determined by a balance between the inertia and buoyancy of the fluid in the current. This long-time behaviour is deduced from a self-similar solution of the shallow-water equations. However, only Fannelop & Waldman and Huppert & Simpson have attempted to develop theories for the initial phase, and nobody has given a physical reason for the observed abruptness of the transition to the second phase.

Fannelop & Waldman's theory, which applies only to releases in deep channels ($h_0/H \ll 1$), predicts that just after release the front depth and the front speed are constant with values $\frac{1}{4}h_0$ and $(g'h_0)^{\frac{1}{2}}$ respectively, where g' is the reduced acceleration of gravity,† h_0 is the initial depth of the released fluid, and H is the total depth of the fluid in the channel. The theory gives no estimates of the duration of the constant-speed phase.

Huppert & Simpson's theory, which applies to the whole range $0 < h_0/H \leqslant 1$, describes the released fluid as collapsing through a series of equal-area rectangles. This theory predicts that just after release the front speed is approximately constant (actually, very slowly decreasing) when $0.075 < h_0/H \leqslant 1$ and that the flow passes directly into the second phase when $h_0/H \leqslant 0.075$. In the former case, the initial front speed has magnitude $\frac{1}{2}(h_0/H)^{-\frac{1}{3}}(g'h_0)^{\frac{1}{2}}$, and the transition to the second phase occurs when the current depth passes through the value $h/H = 0.075$, where h is the (constant) depth of the current.

The aim of the present work is to present detailed observations of instantaneous releases for $0 < h_0/H \leqslant 1$, concentrating on the initial adjustment phase and on the transition to the self-similar phase. Our experiments were performed in a channel of rectangular cross-section, with salt water and fresh water as the two fluids, and were designed to emphasize the inviscid motion. As a framework for discussing the experimental results, we also present numerical solutions of the shallow-water equations for a two-layer fluid.

The key features of our observations are that the current front is initially steady with constant depth and speed for all values of h_0/H in the range $0 < h_0/H \leqslant 1$, and the transition to the second phase occurs when a disturbance generated at the end-wall (or a plane of symmetry) overtakes the front. For h_0/H equal to or slightly less than unity the disturbance has the appearance of an internal hydraulic drop and for smaller values of h_0/H it is a long wave of depression. The measured front speeds were generally slower than predicted by the two theories described above. For the initial phase of collapse, the description of the flow as collapsing through a series of equal-area rectangles appears to be incorrect.

A qualitative description of our observations is given in §2. Some numerical solutions of the shallow-water equations for a two-layer fluid, in which we have incorporated a front condition, are described in §3. The experimental and numerical results are compared and discussed quantitatively in §4.

† $g' = (|\rho_1 - \rho_2|/\rho_2)g$, where g is the acceleration due to gravity, ρ_1 is the density of the fluid in the current, and ρ_2 that of the surrounding fluid.

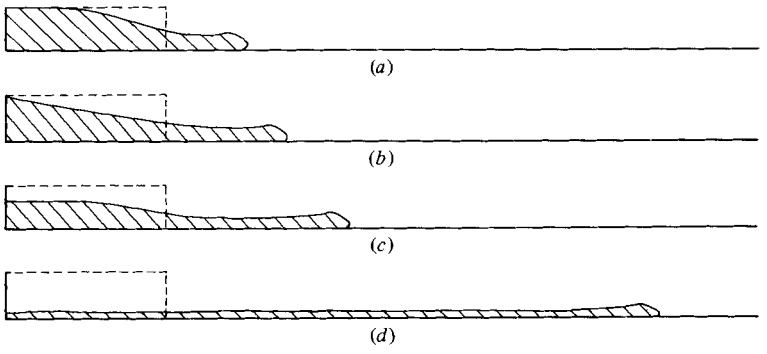

FIGURE 1. Schematic illustrations of the collapse of a volume of heavy fluid with $h_0/H \ll 1$, at four successive times afer release. (*a*), (*b*) and (*c*) are in the adjustment phase, and (*d*) is at the beginning of the inviscid self-similar phase.

2. Experiments

The apparatus used was a Perspex channel of rectangular cross-section, 348 cm long, 50 cm deep and 20.5 cm wide. The channel was filled with tap water to depth h_0 and then a Perspex gate was placed in the channel at a distance x_0 from one of the endwalls. A quantity of cooking salt was dissolved into the water behind the gate to achieve a desired density, and finally more tap water was added to both sides of the gate, if necessary, so that the total depth of the fluid everywhere in the channel was H. The parameter ranges for the density ratio, channel depth, lock depth and lock length were $0.95 \leqslant \rho_2/\rho_1 < 1.00$, 10 cm $\leqslant H \leqslant$ 50 cm, $0 < h_0/H \leqslant 1$, 10 cm $\leqslant x_0 \leqslant$ 60 cm. The experimental procedure was to withdraw the gate suddenly from the channel. The speed of the current and of the hydraulic drop (if present) were measured by recording the times after release at which they crossed equally spaced marks on the Perspex walls.

Our purpose in this section is to describe the qualitative results of the experiments. The quantitative results are presented and discussed in §4.

For $0 < h_0/H \leqslant 0.7$, the observed motion after the removal of the gate is shown schematically in figure 1. Soon after the gate is removed, the fluid from behind the gate forms a gravity current that moves away from the endwall at constant speed and with constant front depth (figure 1*a*). The acceleration from rest to constant speed happens very rapidly, within a few tenths of a second. The gravity current formed in this way has the structure of steady gravity currents as described by Simpson & Britter (1979); in particular, intense mixing between the two fluids is confined to a region just behind the leading edge of the current, the mixed fluid being left behind the head and above the following current. At the same time a long wave of depression propagates along the fluid interface towards the endwall. This wave is reflected by the endwall (figure 1*b*) and propagates away from the wall with speed slightly greater than the speed of the front (figure 1*c*), eventually overtaking the front (figure 1*d*). Thereafter, the front speed, which up until this time had remained constant, decreases roughly as $t^{-\frac{1}{3}}$ until viscous effects become more important than inertial effects, causing the front speed to decrease more rapidly.

Figures 2(*a–c*) are photographs, corresponding to figures 1(*a–c*), of the release of a volume of salt water into fresh water, showing the long wave approaching, being reflected from, and propagating away from, the endwall. In this experiment

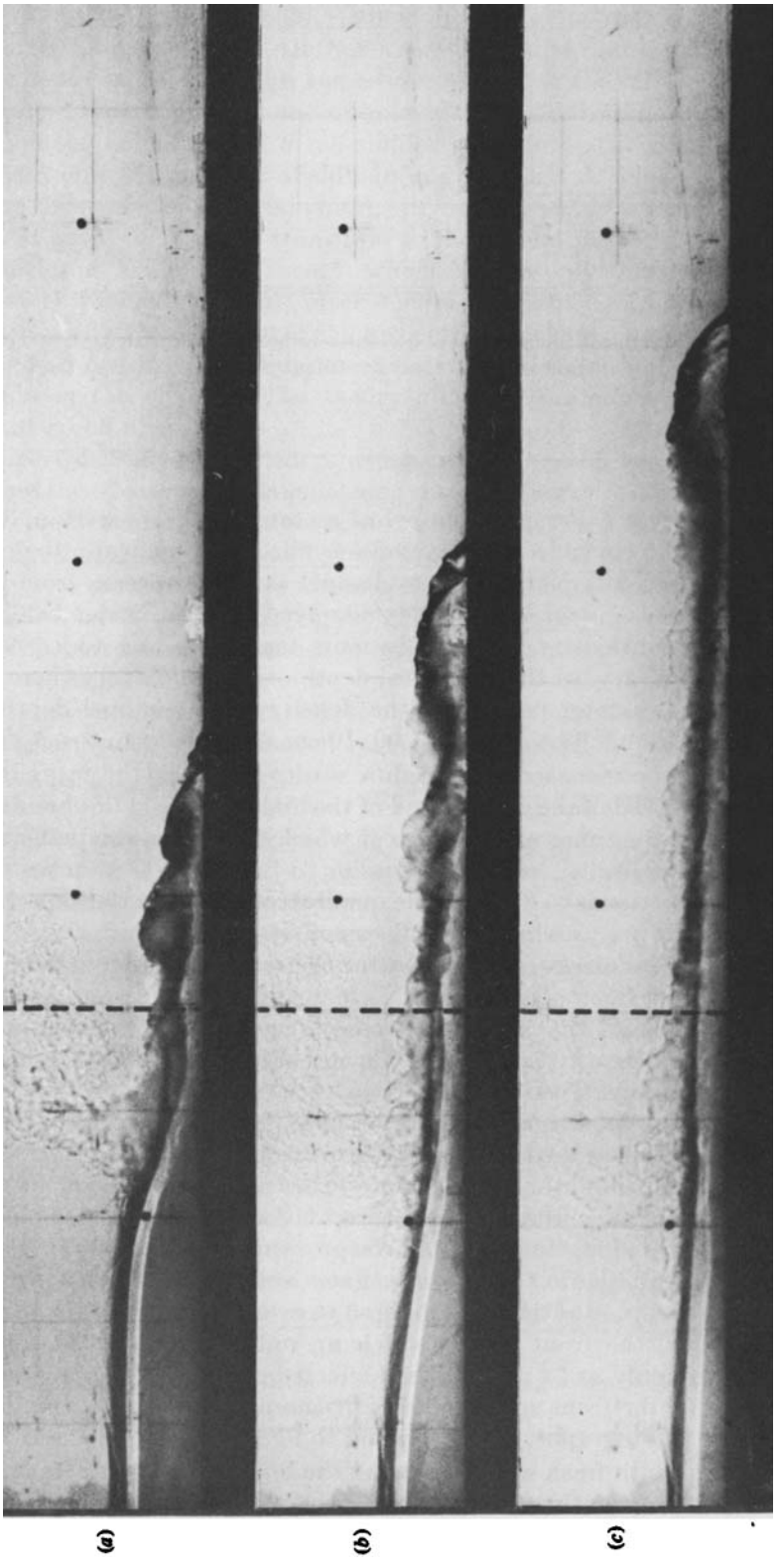

FIGURE 2. Shadowgraph of a volume of salt water with $h_0 = 7$ cm, $H = 49$ cm, $x_0 = 50$ cm, $g' = 47$ cm s^{-2} collapsing into fresh water at approximately 2.2, 3.8 and 6.0 s after release (corresponding to figure 1). The dotted vertical line indicates the position of the lock gate, the endwall is at the far left, and the thin vertical lines are at 10 cm intervals.

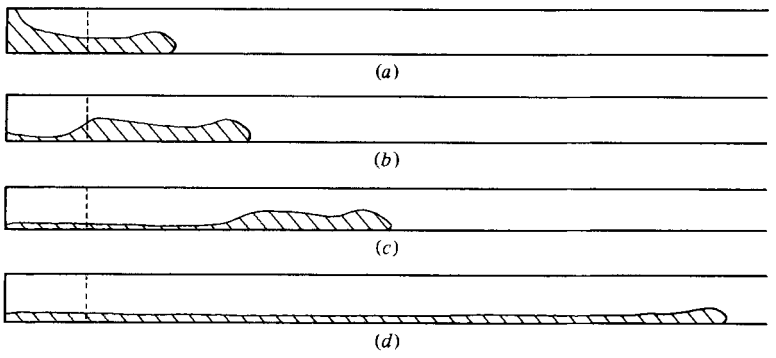

FIGURE 3. Schematic illustrations of the collapse of a volume of heavy fluid with $h_0/H = 1$ at four successive times after release. (*a*), (*b*) and (*c*) are in the adjustment phase, and (*d*) is at the beginning of the inviscid self-similar phase.

$h_0/H = 0.14$ and the front speed was observed to remain constant until the front was about four lock lengths from the endwall.

For $0.8 \lesssim h_0/H \leqslant 1$, the flow is essentially the same as that for smaller values of h_0/H except that the backflow towards the endwall forms an internal hydraulic drop (an abrupt decrease in the interface level – a type of internal bore) at the interface, which as $h_0/H \to 1$ becomes a gravity-current front. It is difficult to determine the exact value of h_0/H at which the transition from a long wave to an hydraulic drop occurs; the best estimate we can give is that it occurs somewhere in the range of $0.7 \leqslant h_0/H \lesssim 0.8$. When the hydraulic drop or gravity current front encounters the endwall, a disturbance that resembles an interfacial hydraulic drop is generated that propagates away from the wall with constant speed, eventually overtaking the front. The reflected hydraulic drop is difficult to observe accurately because it propagates along a mixed layer created by the gravity-current front moving away from the wall. Again, after the front has been overtaken, its speed begins to decrease roughly as $t^{-\frac{1}{3}}$ until viscous effects dominate inertial effects, causing the front speed to decrease more rapidly.

Figure 3 is a schematic illustration of the flow for $h_0/H = 1$. In this case the displaced upper fluid forms a gravity current that propagates towards the endwall (figure 3*a*). When the backflowing current meets the wall a hydraulic drop is generated (figure 3*b*), which propagates away from the wall (figure 3*c*) and eventually overtakes the front (figure 3*d*). Figures 4(*a–c*) are photographs, corresponding to figures 3(*a–c*), of the release of a volume of salt water into fresh water. In this experiment the front was observed to be about ten lock lengths from the endwall when it was overtaken by the bore. This particular case ($h_0/H = 1$) has been discussed briefly by Simpson (1982).

In all the cases discussed above, once the front speed begins to decrease, the gravity current is well described as collapsing through a series of equal-area rectangles. That is, the current depth is roughly uniform along the length of the current, but steadily decreases with time.

3. Analysis

As a framework for discussing the quantitative results of the experiments, we solve an idealized initial-value problem. We consider two-dimensional flow of a two-layer fluid bounded at top and bottom by rigid horizontal planes and at one end by a

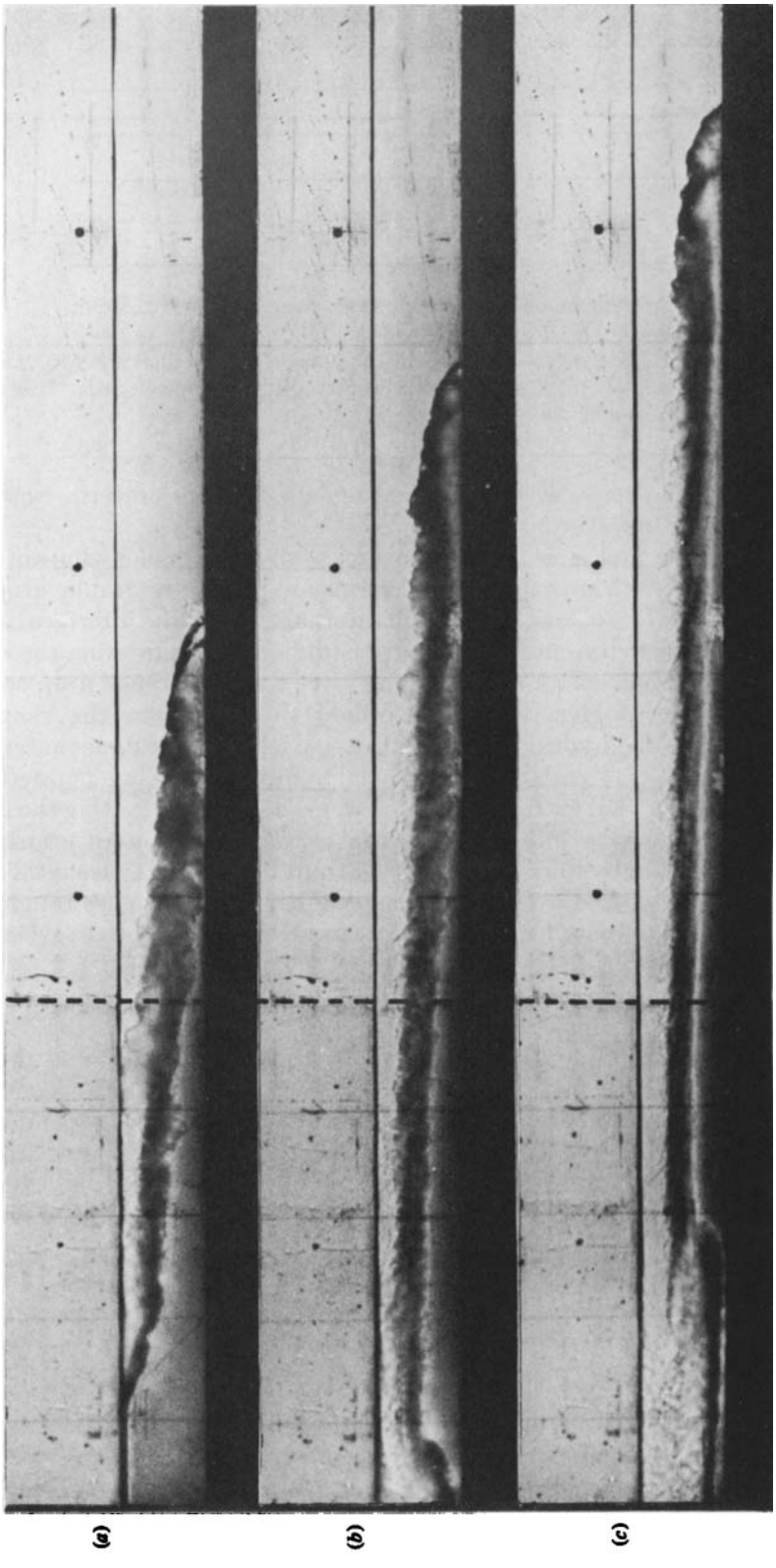

FIGURE 4. Shadowgraphs of a volume of salt water with $h_0/H = H = 7$ cm, $x_0 = 50$ cm, $g' = 47$ cm s^{-2} collapsing into fresh water at approximately 4.7, 7.7 and 10.7 s after release (corresponding to figure 3). The dotted vertical line indicates the position of the lock gate, the endwall is at the far left, and the thin vertical lines are at 10 cm intervals.

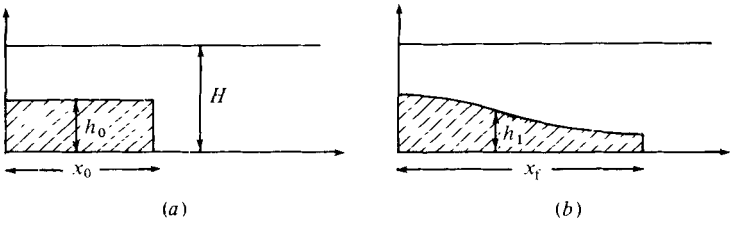

FIGURE 5. Schematic illustration of a constant-volume release in a rectangular channel: (*a*) before release, (*b*) after release.

vertical wall. The two fluids are taken to have slightly different densities, to be inviscid and incompressible and any mixing between them is neglected. The flow is approximated as horizontal and the velocity within each layer as independent of vertical position.

We use a rectangular coordinate system with x-axis along the bottom horizontal plane and y-axis along the endwall. The fluid in the lower layer has density ρ_1, depth h_1 and horizontal velocity u_1, whereas in the upper fluid the same letters are used with subscript 2. Figure 5 is a schematic drawing of the idealized problem under consideration.

3.1. *Governing equations*

The shallow-water equations for a two-layer fluid are

$$\frac{\partial h_1}{\partial t} + \frac{\partial}{\partial x}(u_1 h_1) = 0, \tag{3.1}$$

$$\frac{\partial h_2}{\partial t} + \frac{\partial}{\partial x}(u_2 h_2) = 0, \tag{3.2}$$

$$\frac{\partial u_1}{\partial t} + u_1 \frac{\partial u_1}{\partial x} = -\frac{1}{\rho_1}\frac{\partial p_0}{\partial x} - g\frac{\partial h_1}{\partial x}, \tag{3.3}$$

$$\frac{\partial u_2}{\partial t} + u_2 \frac{\partial u_2}{\partial x} = -\frac{1}{\rho_2}\frac{\partial p_0}{\partial x} - g\frac{\partial h_1}{\partial x}, \tag{3.4}$$

where $p_0(x,t)$ is the pressure at the fluid interface. Equations (3.1) and (3.2) represent conservation of mass in each layer, and (3.3) and (3.4) represent conservation of horizontal momentum in a hydrostatic pressure field.

Since

$$H = h_1(x,t) + h_2(x,t) \tag{3.5}$$

and both velocities vanish at $x = 0$, we deduce from (3.1) and (3.2) that

$$u_1 h_1 + u_2 h_2 = 0. \tag{3.6}$$

Eliminating p_0 from (3.3) and (3.4) and using (3.5) and (3.6) to eliminate h_2 and u_2, we obtain

$$(1+ra)\frac{\partial u_1}{\partial t} + \left[1 - ra\frac{H+h_1}{H-h_1}\right]u_1\frac{\partial u_1}{\partial x} + \left[g' - r(1+a)^3\frac{u_1^2}{H}\right]\frac{\partial h_1}{\partial x} = 0, \tag{3.7}$$

where $a = h_1/(H-h_1)$ and $r = \rho_2/\rho_1$. If in addition we invoke the Boussinesq approximation (setting $r = 1$ except where this ratio multiplies g), (3.7) becomes

$$\frac{\partial u_1}{\partial t} + (1-2a)\,u_1\frac{\partial u_1}{\partial x} + (1-b)\,g'\frac{\partial h_1}{\partial x} = 0, \tag{3.8}$$

where

$$b = \frac{h_1}{H} + \frac{u_1^2}{g'H}\left(1 - \frac{h_1}{H}\right)^{-2}.$$

We use (3.1) and (3.8) to determine $h_1(x,t)$, $u_1(x_1 t)$ (then $h_2(x_1 t)$, $u_2(x_1 t)$ are found from (3.5) and (3.6)) for the initial conditions

$$h_1(x, t=0) = \left\{ \begin{array}{ll} h_0 & (0 \leqslant x \leqslant x_0), \\ 0 & (x_0 < x), \end{array} \right\} \tag{3.9}$$

and the boundary conditions

$$\left.\frac{\partial h_1}{\partial x}\right|_{x=0} = 0, \quad u_1(x=0,t) = 0. \tag{3.10}$$

These boundary conditions make $x = 0$ a plane of symmetry.

We also impose the front condition

$$u_f^2 = \frac{\beta^2}{2}\frac{2 - h_f/H}{1 + h_f/H}(1 - h_f/H)\, g' h_f, \tag{3.11}$$

where $u_f(t)$ is the front speed, $h_f(t)$ is the front depth and β is a dimensionless constant. A front condition is required in our statement of the problem because near the front, where viscous dissipation and vertical accelerations are important, the shallow-water equations are invalid. Essentially, our use of (3.11) means that we are treating the current front similarly to hydraulic jumps in shallow-water flow. With $\beta^2 = 2$, (3.11) gives the theoretical front speed derived by Benjamin (1968), based on the bulk conservation of mass and momentum, for the steady propagation of an infinitely long cavity in a rectangular tube. We have left β to be determined by experiments, but expect it to be of order one.

In the limit $h_1/H \to 0$, (3.1) and (3.8) reduce to the familiar one-layer shallow-water equations and (3.11) becomes

$$u_f^2 = \beta^2 g' h_f. \tag{3.12}$$

Fannelop & Waldman (1972) and Hoult (1972) found that for constant-volume currents this reduced set of equations has a self-similar solution given by

$$h_1(x,t) = \tfrac{1}{9} g' \alpha^2 t^{-\frac{2}{3}}\left[\eta^2 + \frac{4-\beta^2}{\beta^2}\right], \tag{3.13}$$

$$u_1(x,t) = \tfrac{2}{3}\alpha t^{-\frac{1}{3}}\eta, \tag{3.14}$$

where

$$\alpha = \left[\frac{27\beta^2 g' x_0 h_0}{12 - 2\beta^2}\right]^{\frac{1}{3}}, \quad \eta = \frac{x}{x_f(t)}, \tag{3.15}$$

and $x_f = \alpha t^{\frac{2}{3}}$ is the front position. Comparing these results with experiments, Fannelop & Waldman and Hoult determined that $\beta^2 \approx 1.0$ and 1.4 respectively.† For long time, but not so long that viscous effects become more important than inertial effects, we expect the solutions of our initial-value problem to approach this self-similar solution. Indeed, we have already noted in §2 that the observed front speed (that is, $\mathrm{d}x_f/\mathrm{d}t$) eventually decreases at $t^{-\frac{1}{3}}$. Our main interest is in how this limiting form is approached.

† Note that Fannelop & Waldman (1972) consider β^2 to be a function of time, with $\beta^2 = 4$ for early time and $\beta^2 = 1$ for late time. However, they had no experimental observations supporting their early-time theory.

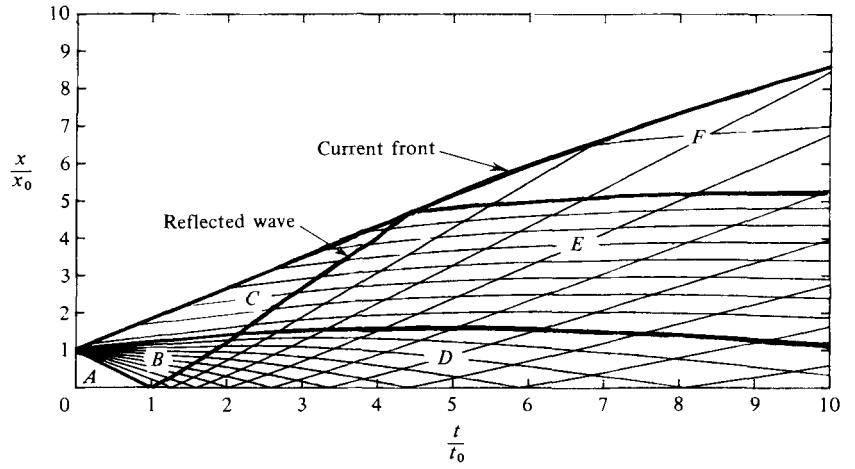

FIGURE 6. The characteristic diagram for the case with $h_0/H = 0$ and $\beta^2 = 2$. The labelled regions in the diagram are: (*A*) region of constant state adjoining the endwall at $x = 0$; (*B*) centred simple-wave region; (*C*) region of constant state at front of current; (*D*) complex wave region adjoining the wall; (*E*) simple-wave region; (*F*) complex wave region at current front. $t_0 = x_0/(g'h_0)^{\frac{1}{2}}$ is a timescale.

3.2. *Method of solution*

We used the method of characteristics to solve the initial-value problem formulated in §3.1. As described (for example) in Ames (1965, pp. 416–422), the solution of the partial differential equations (3.1) and (3.8) is equivalent to the solution of the ordinary differential equations

$$h_1 \frac{\mathrm{d}u_1}{\mathrm{d}h_1} - (1-2a)\,u_1 + \lambda_\pm = 0, \tag{3.16}$$

along the characteristic directions specified by

$$\frac{\mathrm{d}x}{\mathrm{d}t} = \lambda_\pm, \tag{3.17}$$

where

$$\lambda_\pm = u_1(1-a) \pm [u_1^2 a^2 + g'h_1(1-b)]^{\frac{1}{2}}. \tag{3.18}$$

The numerical algorithm we used to solve (3.16) and (3.17) is outlined in Ames (1965, pp. 435–437). The method of characteristics is particularly convenient for this problem because the position of the front, where (3.11) is applied, is computed explicitly.

The characteristic diagram for the case with $h_0/H = 0$ and $\beta^2 = 2$ is shown in figure 6. This diagram is typical of the characteristic diagrams for other values of h_0/H and β. The diagram shows that initially the flow consists of a centred simple expansion wave that connects a region of constant state at the front of the current to another region of constant state adjoining the endwall at $x = 0$ (using the terminology of hyperbolic waves). This description of the initial motion for $h_0/H = 0$ has also been given by Abbott (1961) and Fannelop & Waldman (1972). The diagram also shows the reflection of the centred expansion wave from the endwall. As soon as the first characteristic of the reflected wave intersects the curve representing the front position, which up to this point is a straight line, the front curve begins to bend towards the time axis, indicating that the front speed is decreasing.

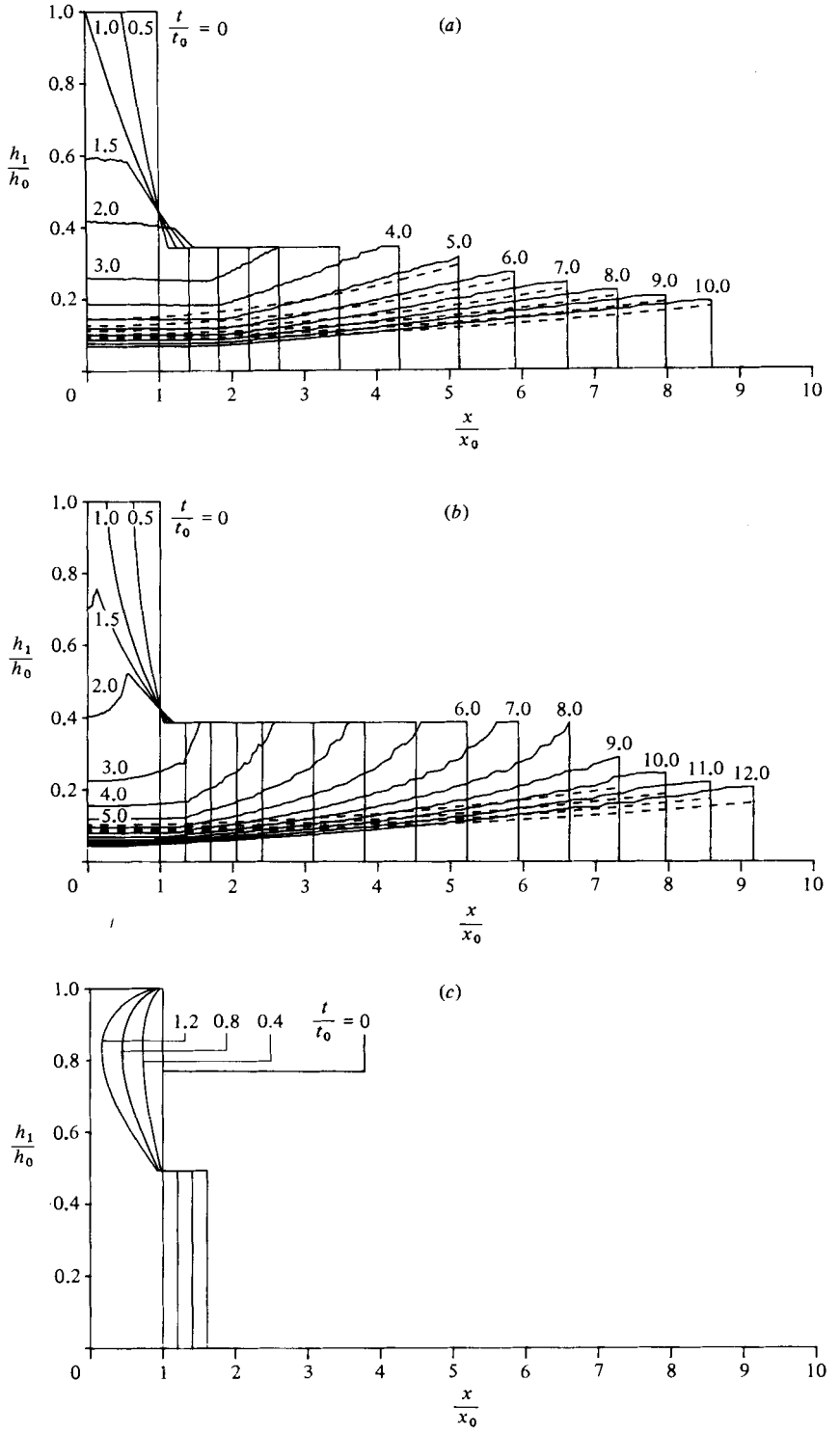

FIGURE 7. The theoretical depth profiles of collapsing constant volumes of fluid at several times after release: ——, computed using method of characteristics, – – – –, self-similar solutions (3.13). (*a*) $h_0/H = 0$, (*b*) $h_0/h = \frac{1}{2}$, (*c*) $h_0/H = 1$, all with $\beta^2 = 2$.

Solutions for the current profile h_1 for several times after release are shown in figures 7 (*a–c*), for $h_0/H = 0, \frac{1}{2}$ and 1 respectively, again with $\beta^2 = 2$. Also shown (as dashed lines) in the first two of these figures are the profiles given by (3.13); these self-similar solutions, which have only been drawn for times after the computed front speed begins to decrease, are plotted with shifted time origins so that their horizontal length equals that of the numerically computed profiles. It can be seen that the computed solutions have the essential features of the flow, as described in §2, and as shown in figures 1–4. For small h_0/H the computed simple wave, as it approaches the endwall, has an interface slope that decreases with time and which generates a weak wave when it is reflected by the endwall. As $h_0/H \to \frac{1}{2}$, the computed simple wave has a very steep interface slope that does not decrease with time and that generates a stronger wave when it interacts with the endwall. For $h_0/H > \frac{1}{2}$, the computed profiles are multivalued functions of position, as shown in figure 7 (*c*). The range of h_0/H for which this occurs is independent of β. Clearly, the multivalued solutions are unphysical and suggest that for $h_0/H > \frac{1}{2}$ the backflowing simple wave should be replaced in the analysis by an interfacial hydraulic drop.

Physically, the backflowing simple wave is stronger for larger values of h_0/H because the fluid in the upper layer must travel at greater speed the shallower the upper-layer depth is in relation to the lower-layer depth. The model calculations indicate that this trend results in the formation of an interfacial hydraulic drop for $h_0/H > \frac{1}{2}$, whereas in our experiments we observe no indication of a hydraulic drop until $h_0/H > 0.7$. There are several possible reasons for this discrepancy, but the most likely are mixing between the two fluids and the smooth velocity profile in the experiments (as opposed to the discontinuous profile in the model).

We attempted to use the approximate theory of Yih & Guha (1955) to incorporate a hydraulic drop into our calculations. Our idea was to determine the speed and strength of the hydraulic drop that matched up with the speed and depth of the current front that satisfied (3.11), and then compute the speed and depth of the reflected hydraulic drop. The front speed would begin to decrease when the reflected hydraulic drop overtook the front. However, because our results are not entirely satisfactory, we choose not to present them. The theory of jumps and drops in two-layer fluids is not well developed. A more complete study of our problems will have to await further developments in this theory.

4. Results and discussion

Figure 8 is a plot of the front position and the bore position, for the case $h_0/H = 1$, as functions of time after release. Most of the data in this plot are from our experiments, but we have also included one set of results each from Keulegan (1957) and Huppert & Simpson (1980).† The solid lines in the plot are straight-line fits to the data at early time. It is quite clear that both the front and the bore travel at constant speed initially and that the front speed begins to decrease at the point where the two lines intersect. The constant speeds of the front and the bore were estimated as the slopes of these lines.

Similar plots were made for other values of h_0/H, and the front speeds estimated from these plots are shown in figure 9. The front speed scaled by $(g'h_0)^{\frac{1}{2}}$ is seen to decrease (almost linearly with h_0/H) from about 0.7 for $h_0/H = 0$ to about 0.5 for

† Huppert & Simpson (1980) gave no results for the bore position. Although Keulegan (1957) does not mention the bore, it appears in his plots of the gravity-current profile; we obtained the data for the bore position shown in figure 8 from these profile plots.

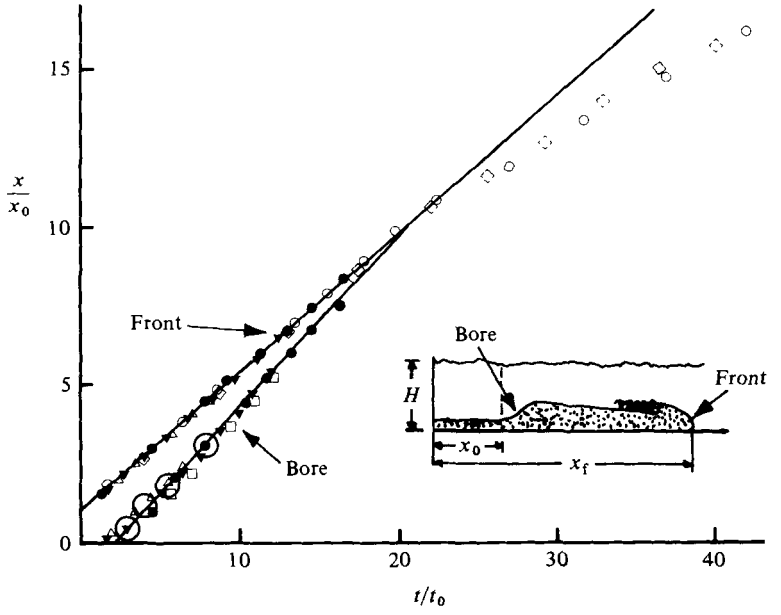

FIGURE 8. The front position and bore position as functions of time after release with $h_0/H = 1$: ——. straight-line fits to the data at early time; □, $h_0 = 10$ cm, $x_0 = 40$ cm, $g' \approx 9.8$ cm/s²; △, 10 cm, 60 cm, 9.8 cm/s²; ▼, 10 cm, 50 cm, 19.6 cm/s²; ●, 20 cm, 40 cm, 39.2 cm/s²; ○, 15 cm, 30 cm, 39.2 cm/s²; ◇, 29.8 cm, 20.2 cm, 11.2 cm/s² (Huppert & Simpson); ○, $h_0 = 26$ cm, $x_0 = 188$ cm, $g' = 19.6$ cm/s² (Keulegan 1957).

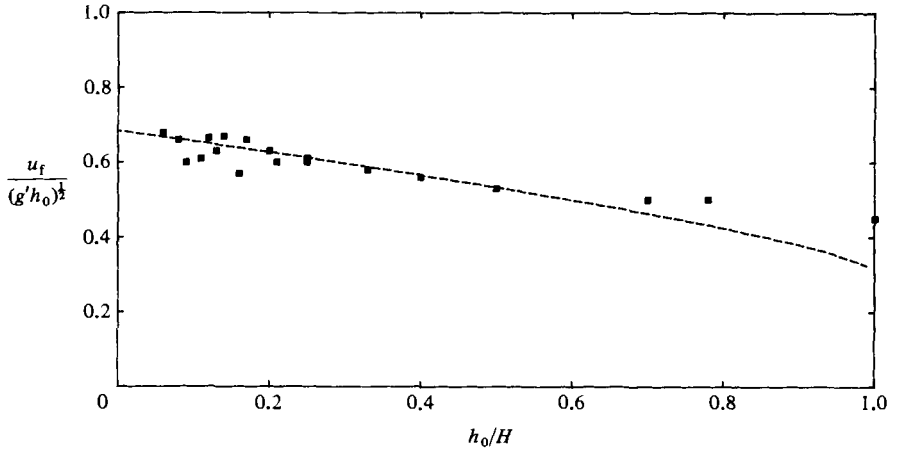

FIGURE 9. The front speed u_f during the initial phase of collapse plotted as a function of h_0/H: ■, experiments; ——, theory with $\beta = 1.0$.

$h_0/H = 1$. Also shown in this plot is a curve representing the constant front speeds computed as described in § 3, with $\beta^2 = 1$. As discussed before, the theory is only valid for $0 < h_0/H \leqslant \frac{1}{2}$, and in this range the agreement is excellent. Contrary to the theory of Fannelop & Waldman (1972), we found that $\beta^2 = 1$ gave the best agreement with the experimental results for both early and late time.

The measured gravity-current front depths during the initial stage of collapse are shown in figure 10 for various values of h_0/H. As described by Britter & Simpson

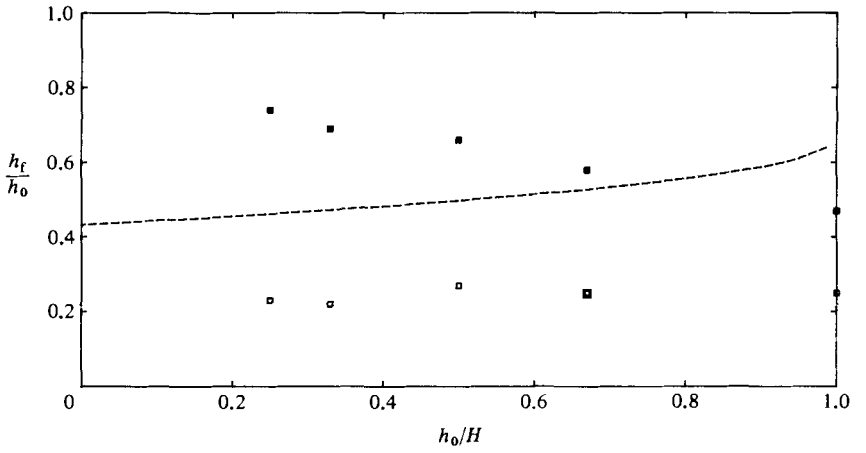

FIGURE 10. The front depth during the initial phase of collapse plotted as a function of h_0/H: □, the measured depth h_4 of the unmixed current layer; ■, the measured total depth h_3+h_4 of the current behind the front; ----, theoretical front depth h_f with $\beta^2 = 1.0$.

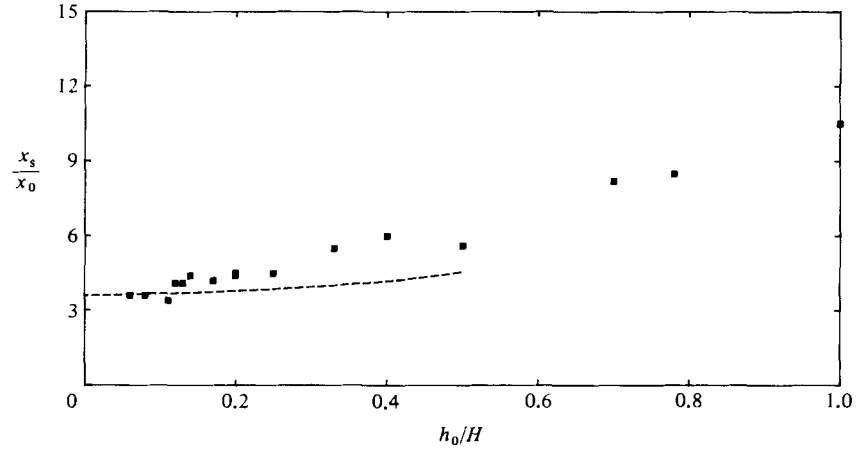

FIGURE 11. The length x_s of the gravity current when its front speed begins to decrease: ■, experiments; ----, theory with $\beta^2 = 1.0$.

(1978), gravity currents in miscible fluids consist of a lower layer of unmixed heavy fluid overlaid by a layer of mixed lighter fluid. They denote the depth of the mixed layer as h_3 and that of the unmixed layer as h_4. We have plotted h_4 and h_3+h_4 in the figure. Also plotted is a curve representing the computed front depth. In the range $0 < h_0/H \leqslant \frac{1}{2}$, the computed depths are about halfway between the two measured depths, as expected since the model assumes there is no mixing and the total mass of the released fluid is conserved.

The length x_s of the gravity current when the front speed begins to decrease is plotted in figure 11 as a function of h_0/H. These points are not direct measurements but estimates from plots of the measured front positions versus time. The length x_s/x_0 is seen to increase (almost linearly with h_0/H) from about 3 for $h_0/H = 0$ to about 10 for $h_0/H = 1$. Also shown in this plot is a curve representing the computed horizontal position (with $\beta^2 = 1$) where the reflected wave overtakes the current front, in the range $0 < h_0/H \leqslant \frac{1}{2}$. The computed results are in fair agreement with the data; we

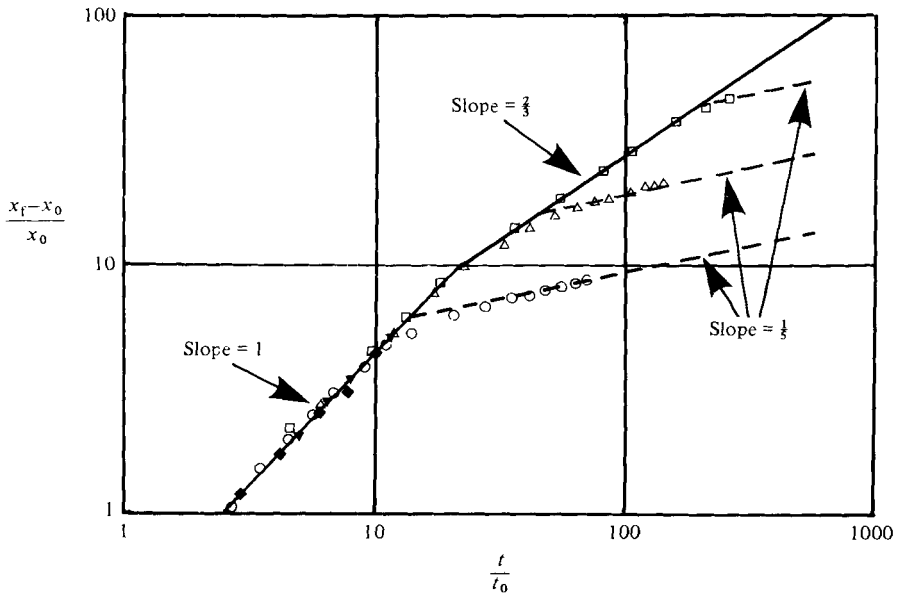

FIGURE 12. The front position as a function of time for different releases with $h_0/H = 1$: ○, $x/x_0 = 6$; ◆, 10; △, 12; ▼, 18; □, 25. The initial adjustment phase is represented by the line with slope 1, the inviscid self-similar phase by the line with slope $\frac{2}{3}$ and the viscous self-similar phase by slope $\frac{1}{5}$.

expect the computed results to be short of the experimental estimates because the laboratory current must travel a short distance before we can detect that its front speed is decreasing.

All the results we have presented so far are dependent upon inertial effects being more significant than viscous effects. Viscous effects may become more important beginning in either the first or second phase of collapse. Huppert (1982) estimates that a gravity current moving along a rigid boundary will have length of the order of

$$x_* = (x_0^5 h_0^5 g'/\nu^2)^{\frac{1}{7}}, \tag{4.1}$$

when viscous effects begin to dominate inertial effects, where ν is the kinematic viscosity of the fluid in the current. Assuming a balance between buoyancy and viscous forces in the current, Huppert, following Barenblatt (1952), derives a self-similar solution of the lubrication equations that gives the front speed decreasing as $t^{-\frac{4}{5}}$. Figure 12 is a plot of the measured front positions as a function of time for several lock-release experiments with $h_0/H = 1$ but with different values of x_*/x_0. Both scales in the plot are logarithmic, so the inviscid initial adjustment phase is represented by a straight line with slope 1, the inviscid self-similar phase by a straight line with slope $\frac{2}{3}$, and the viscous self-similar phase by straight lines with slope $\frac{1}{5}$.† The plot shows that the measured points follow the inviscid theory until $x_f \approx x_*$, and then they approach the predicted viscous behaviour. Similar results were obtained for other values of h_0/H. Therefore to ensure that both inviscid phases are obtained in the experiments, initial conditions must be chosen such that $x_* \gg x_s$.

† Simpson (1982, p. 220) mistakenly described the length of the current as increasing as $t^{\frac{1}{5}}$ in the viscous self-similar phase. The experimental results of Barr (1967), when made non-dimensional and replotted, agree with the description we have given here.

5. Concluding remarks

We have presented experimental results for the release of a heavy fluid in a rectangular channel and have given an interpretation of these results in terms of shallow-water theory for a two-layer fluid. Our interpretation gives a qualitative understanding of the results for $0 < h_0/H \leqslant 1$, but is quantitatively accurate only for $0 < h_0/H < \frac{1}{2}$.

Although we have restricted our attention to the release of heavy fluids in rectangular channels, the qualitative aspects of our interpretation of these results apply in many different situations. For example, a volume of air collapsing into water in a closed horizontal tube of rectangular cross-section forms a steady air cavity front that travels along the top of the tube. The cavity front speed remains constant until it is overtaken by a hydraulic jump that was generated at the tube end. We have performed experiments with $h_0/H = 1$ and found that the cavity is about $8x_0$ long before its front speed begins to decrease. Using Benjamin's (1968) steady-cavity theory, with corrections for surface tension suggested by Wilkinson (1982), and the standard theory of hydraulic jumps, we obtain a theoretical length of $8.3x_0$.

An axisymmetric flow resulting from the release of a cylindrically shaped volume of heavy fluid also passes through two phases. We have performed experiments simulating this type of flow by releasing heavy fluid in a sector tank. In the initial phase, the front speed is nearly constant and in the second phase the front speed decreases as $t^{-\frac{1}{2}}$, as expected from self-similar solutions of the axisymmetric shallow-water equations.

We are grateful to H. E. Huppert, N. H. Thomas and I. R. Wood for helpful comments on a draft of this paper. We also thank the referees for several suggestions that lead to substantial improvements of the manuscript. We acknowledge financial support from the National Environmental Research Council (JWR) and the Science Research Council and Central Electricity Generating Board (JES).

REFERENCES

ABBOTT, M. B. 1961 On the spreading of one fluid over another. II. *Houille Blanche* **16**, 847–856.

AMES, W. F. 1965 *Nonlinear Partial Differential Equations in Engineering*. Academic.

BARENBLATT, G. I. 1952 Concerning some nonstationary motions of liquid and gas in a porous medium. *Prikl. Mat. Mek.* **16**, 67–78 (in Russian).

BARR, D. I. H. 1967 Densimetric exchange flows in rectangular channels. *Houille Blanche* **22**, 619–631.

BENJAMIN, T. B. 1968 Gravity currents and related phenomena. *J. Fluid Mech.* **31**, 209–248.

BRITTER, R. E. & SIMPSON, J. E. 1978 Experiments on the dynamics of a gravity current head. *J. Fluid Mech.* **88**, 233–240.

FANNELOP, T. K. & WALDMAN, G. D. 1972 Dynamics of oil slicks. *AIAA J.* **10**, 506–510.

FAY, J. A. 1969 The spread of oil slicks on a calm sea. In *Oil on the Sea* (ed. D. P. Hoult), pp. 43–63. Plenum.

HOULT, D. P. 1972 Oil spreading on the sea. *Ann. Rev. Fluid Mech.* **4**, 341–368.

HUPPERT, H. E. 1982 The propagation of two-dimensional and axisymmetric viscous gravity currents over a rigid horizontal surface. *J. Fluid Mech.* **121**, 43–58.

HUPPERT, H. E. & SIMPSON, J. E. 1980 The slumping of gravity currents. *J. Fluid Mech.* **99**, 785–799.

KEULEGAN, G. H. 1957 An experimental study of the motion of saline water from locks into fresh water channels. *Natl Bur. Stand. Rep.* 5168.

O'BRIEN, M. P. & CHERNO, J. 1934 Model law for motion of salt water through fresh. *Trans. ASCE* **99**, 576–594.

SIMPSON, J. E. & BRITTER, R. E. 1979 The dynamics of the head of a gravity current advancing over a horizontal surface. *J. Fluid Mech.* **94**, 477–495.

SIMPSON, J. E. 1982 Gravity currents in the laboratory, atmosphere, and ocean. *Ann. Rev. Fluid Mech.* **14**, 213–234.

WILKINSON, D. L. 1982 Motion of air cavities in long horizontal ducts. *J. Fluid Mech.* **118**, 109–122.

YIH, C. S. 1947 A study of the characteristics of gravity waves at a liquid interface. M. S. thesis, State University of Iowa. [Also Yih, C. S. 1980 *Stratified Flows*. Academic.]

YIH, C. S. & GUHA, C. R. 1955 Hydraulic jumps in a fluid system of two layers. *Tellus* **7**, 358–366.